# Computer Simulation of the Dynamics of Neutral and Charged Dendrimers

**Sergey V. Lyulin,[†] Anatolij A. Darinskii,[†] Alexey V. Lyulin,*[,‡] and M. A. J. Michels[‡]**

*Institute of Macromolecular Compounds, Russian Academy of Sciences, Bolshoj Prospect 31, St. Petersburg 199004, Russia, and Group Polymer Physics, Eindhoven Polymer Laboratories and Dutch Polymer Institute, Technische Universiteit Eindhoven, P.O. Box 513, 5600 MB Eindhoven, The Netherlands*

*Received November 28, 2003; Revised Manuscript Received April 8, 2004*

ABSTRACT: Dynamic properties of dilute solutions of neutral and charged dendrimers with explicit excluded-volume, electrostatic, and hydrodynamic interactions have been investigated by Brownian dynamics simulation. Three different types of motions in dendrimers up to $g = 5$ generations have been considered: the motion of a dendrimer as a whole; the size and shape fluctuations (pulsations); the local reorientations of the individual monomers. The influence of the excluded-volume, electrostatic, and hydrodynamic interactions on these motions has been studied. The characteristic relaxation times have been compared with the theoretical predictions of the Rouse and Zimm models. The self-diffusion of a dendrimer can be described with the help of the preaveraged Zimm approach, and a dendrimer may be considered as an impenetrable sphere with the hydrodynamic radius $R_h$. For both neutral and charged dendrimers the hydrodynamic radius is smaller than the gyration radius $R_g$. The dynamics of the size fluctuations for a dendrimer with rigid spacers differs significantly from the theoretical predictions for a dendrimer with flexible spacers. The relaxation of these fluctuations is weakly sensitive to the presence of the hydrodynamic interactions, and the behavior of a dendrimer is close to that of an elastic body in a viscous medium. The local orientational mobility of individual monomers is significantly influenced by the ionization of the terminal groups.

## 1. Introduction

During the last two decades dendrimers have attracted considerable interest because of their unconventional properties related to their architecture and regularity, and the efforts to understand the solution and bulk behavior of dendrimers have been intensified. The most widespread are water-soluble dendrimers which contain charged groups. These ionized dendrimers are used for different applications, in particular in host−guest systems (as delivery vehicles, for medical uses, etc.).[1−4]

The majority of theoretical and simulation efforts is devoted to the investigation of the equilibrium properties of neutral dendrimers. It was shown that, contrary to the predictions of de Gennes and Hervet,[5] even in a good solvent dendrimers have rather compact structures, with density decreasing from the core to the periphery. The terminal groups are not fixed on the dendrimer surface but distributed through the whole volume. Welch and Muthukumar[6,7] studied some statistical properties of charged dendrimers by Monte Carlo (MC) simulations. It was shown that such dendrimers should undergo significant change of their size and density profile by a change of the solution salt concentration. The terminal groups are shifted to the periphery by decrease of the salt concentration. MC simulation of the complex formation between a charged dendrimer and a linear polyelectrolyte have been also carried out by Welch and Muthukumar.[7] However, the MC method[6,7] allows one to study only equilibrium properties of dendrimers.

The dynamics of dendrimers determines their use in potential applications. Dynamical properties of dendrimers are experimentally investigated by small-angle neutron-scattering experiments, NMR, and other methods.[8−11] To our knowledge there are only few theoretical studies related to the dynamics of dendrimers in solution[12−14] in which the Rouse model for spacers connecting two consequent branching points has been used. The Rouse model supposes that the spacer length is long compared to the bond length. However, in real dendrimers the spacers contain only few monomers and should be considered as rather rigid elements. The second, and even more important simplification used, for example by Cai and Chen,[12] is neglecting of the excluded-volume interactions. As was shown by previous studies,[13,15−17] these interactions strongly influence the structure of dendrimers. The effect of the excluded-volume and electrostatic interactions in charged dendrimers on their internal dynamics is expected to be also significant.

Including the excluded-volume, electrostatic, and hydrodynamic interactions (HI) into the analytical dynamic theory of dendrimers leads to a significant complication of the equations of motion. Chen and Cai[13] used MC computer simulations to carry out the thermodynamical averaging and Rouse and Zimm models with hard-core repulsive potential for excluded-volume interactions to overcome these difficulties. With the help of the preaveraged HI approximation they calculated different internal relaxation times and the diffusion coefficient of a dendrimer as a whole. However, the linearized version of the Langevin equation, used by Chen and Cai,[13] leads in some cases to the wrong result, in particular, for the relaxation time of the squared radius of gyration. The direct way to overcome these difficulties is to use computer simulation of a dendrimer dynamics.

To our knowledge there exist only few papers where simulation of dendrimer dynamics was carried out

* To whom correspondence should be addressed. E-mail: a.v.lyulin@tue.nl.
[†] Russian Academy of Sciences.
[‡] Technische Universiteit Eindhoven.

10.1021/ma0357927 CCC: $27.50 
Published on Web 05/21/2004

explicitly. Murat and Grest[16] have performed a molecular dynamics (MD) simulation of a coarse-grained model of neutral dendrimers of generations $g = 5-8$ in solvents of varying quality. The main attention was devoted to the study of equilibrium properties of dendrimers, such as a squared radius of gyration and radial monomer density, as functions of generation number and solvent quality. As to dynamical properties, only the relaxation of the correlation function for the squared radius of gyration, $R_g^2$, was considered. The simulated dependence of the relaxation times on the generation number was very noisy, and it was difficult to draw any quantitative conclusions.

Karatasos et al.[17] performed MD simulation of coarse-grained models of $AB_2$-dendrimers. Dendrimers of generations $g = 3-6$ in an explicit solvent were considered. Excluded-volume interactions were described by the Lennard-Jones potential with parameter, corresponding to the $\theta$-solvent of the linear chain. Translational diffusion, global reorientational motions, and local segmental dynamics have been investigated. Atomistic MD simulations of the PAMAM dendrimer at several pH conditions, with explicit water molecules and without water, were performed by Lee at al.[18] Only structural characteristics were studied in their paper. The necessity to consider the explicit solvent in MD simulations of dendrimers in solution restricts significantly the scales of motions under study.

Brownian dynamics (BD) represents a compromise allowing one to extend time and length scales of simulated motions.[19−22] In BD simulations the solvent is considered as an effective viscous continuum. In that way it is possible to decrease the number of simulated particles. In many cases it is possible also to neglect the inertial term in equations of motion and increase the value of the integration time step. In this paper the BD method is used to simulate the dendrimers with explicit excluded-volume, electrostatic, and hydrodynamic interactions. Statistical properties of neutral and charged dendrimers in dilute solution were studied in detail in our previous paper.[23] The squared radius of gyration $R_g^2$, the fractal dimension $d_f$, the radial-density distribution functions $\rho(r)$, and the density distribution of terminal beads $\rho_T(r)$ were calculated.[23] Our results show that dendrimer can be considered as a fractal object with the fractal dimension depending both on its generation number and spacer length.

The main goal of this study is to investigate the dynamical properties of neutral and charged dendrimers in dilute solution. Dynamic characteristics of dendrimers corresponding to the different time and length scales, such as translational self-diffusion, characteristic time of the fluctuations of the radius of gyration, and orientational autocorrelation functions in solutions of different ionic strength, have been simulated. The study of these dynamic properties helps to understand the hierarchy of the relaxation processes in the considered systems. Simulation results have been compared with those produced by previous computer simulation studies and with theoretical results based on the Rouse model.[12,13]

The paper is organized as follows. In section 2 the model and the method of simulation are reported. In section 3 the different relaxation processes (global, elastic, and local) in dendrimers are discussed. The influence of the hydrodynamic and the electrostatic interactions is analyzed. Finally, some conclusions are made in section 4.

## 2. Model of Dendrimer and Simulation Algorithm

We consider the bead-rod freely jointed model of dendrimers identical with that used in our previous papers.[19−23] No valence-angle and torsional potentials are taken into consideration. Dendrimers with three functional groups are studied. Dendrimer generations start from the generation $g = 0$ consisting of 4 beads including the core. The total number $N$ of beads in a dendrimer with $g$ generations is defined by the following equation:

$$N = 3s(2^{g+1} - 1) + 1 \tag{1}$$

Here $s$ is the spacer length between the branching points. The case $s = 1$ is considered here. Dendrimers up to generation $g = 5$ ($N = 190$) have been simulated.

The dendrimer is represented as a system of beads with friction coefficient $\zeta$, connected by rigid bonds of length $l$. The finite-difference numerical scheme implemented here is based on the Ermak−McCammon equation[19−24]

$$\vec{r}_i = \vec{r}_i^{\,0} + \frac{\Delta t}{k_b T}\sum_j D_{ij}^{\,0}\vec{F}_j^{\,0} + \vec{\Phi}_i^{\,0}(\Delta t) \tag{2}$$

where $\vec{r}_i^{\,0}$ is the position vector of the $i$th particle ($i = 0$ corresponds to the core) before the integration step, $k_b$ is the Boltzmann constant, $T$ is the absolute temperature, $D_{ij}^{\,0}$ is the diffusion tensor, and $\Delta t$ is the integration step.

The solvent is considered as a structureless viscous continuum with chain-solvent collisions mimicked by an random force $\vec{\Phi}^0$ (white noise):

$$\langle\vec{\Phi}^0\rangle = 0 \tag{3}$$

$$\langle\vec{\Phi}_i^{\,0}(\Delta t)\vec{\Phi}_j^{\,0}(\Delta t)\rangle = 2\Delta t D_{ij}^{\,0} \tag{4}$$

The complete force $\vec{\Phi}_j^{\,0}$ in the eq 2 acting on the $j$th bead is the sum of the forces due to the rigid constraints and potential forces:

$$\vec{F}_j^{\,0} = -\sum_{k=1}^{N}\mu_k\left(\frac{\partial\sigma_k}{\partial\vec{r}_j}\right)_{r^0} - \partial U^{LJ}/\partial\vec{r}_j^{\,0} - \partial U_j^{\,C}/\partial\vec{r}_j^{\,0} \tag{5}$$

Here $\sigma_k$ is the equation of the $k$th rigid constraint and $\mu_k$ is the corresponding Lagrange multiplier.

Excluded-volume interactions are defined by the repulsive Lennard-Jones potential $U^{LJ}$ corresponding to the athermal solvent, with the cutoff distance $r_{cut} = 2.5\sigma$ and parameters $\sigma = 0.8l$ and $\epsilon_{LJ} = 0.3k_bT$:

$$U^{LJ}(r_{ij}) = 4\epsilon_{LJ}\left(\frac{\sigma}{r_{ij}}\right)^{12} - 4\epsilon_{LJ}\left(\frac{\sigma}{r_{cut}}\right)^{12} \tag{6}$$

We simulated dendrimers in which only terminal groups are ionized possessing the same charge $ze$. Since the number of terminal groups increases with generation number as $\sim 2^g$, their ionization leads to rather large surface charge density. Nevertheless, high degrees of ionization of terminal groups were observed experimentally for aqueous solutions of poly(propylene imine)[25] and poly(amidoamine)[26] dendrimers.

The electrostatic interactions $U_j^C$ between the $j$th and all other charged beads are approximated by the De-

bye−Hückel potential

$$\frac{U_j^{\mathrm{C}}}{k_{\mathrm{b}}T} = \lambda_{\mathrm{B}} z^2 \sum_{i=1}^{N_{\mathrm{T}}} \frac{\exp(-r_{ij}/r_{\mathrm{D}})}{r_{ij}} \tag{7}$$

where $N_{\mathrm{T}}$ is a number of terminal beads, $r_{ij}$ is the distance between the $i$th and $j$th terminal beads, and $\lambda_{\mathrm{B}}$ is the Bjerrum length characterizing the strength of the Coulomb interactions in a medium with dielectric constant $\epsilon$,

$$\lambda_{\mathrm{B}} = \frac{e^2}{4\pi\epsilon k_{\mathrm{b}}T} \tag{8}$$

The value of $\lambda_{\mathrm{B}}$ in water at room temperature is about 7 Å and is close to the segment length for a usual flexible polymer. Therefore, we could put $\lambda_{\mathrm{B}} = l$ without loss of practical generality. $r_{\mathrm{D}}$ in the eq 7 is the Debye length, which depends on valencies and concentrations of ions in the solution,

$$1/{r_{\mathrm{D}}}^2 = 4\pi\lambda_{\mathrm{B}} \sum_i c_i {z_i}^2 \tag{9}$$

$c_i$ and $z_i$ are the concentration and the valence of the $i$th ion, respectively. Two cases, $z = 0$ (neutral dendrimer) and $z = 1$ (charged dendrimer) have been simulated. We have considered the same values for the Debye length, $r_{\mathrm{D}}$, as used by Welch and Muthukumar:[7] $r_{\mathrm{D}} = 0.8$, 1.54, 8.96, and 100, corresponding to different values of the salt concentration in water (from 0.28 M to the solution with almost nonscreened electrostatic interactions).

HI are taken into account explicitly with the help of the Rotne−Prager−Yamakawa tensor.[19,21,27] The diagonal elements of the diffusion tensor $D_{ii}$ are defined as

$$D_{ii}^{(\alpha\beta)0} = (k_{\mathrm{b}}T/\zeta)\delta_{\alpha\beta} \tag{10}$$

where α and $\beta$ are Cartesian components and $\delta_{\alpha\beta}$ is the Kronecker symbol. Nondiagonal elements of the diffusion tensor are represented as

$$D_{ij}^{\alpha\beta} = h(\pi/3)^{1/2}(3k_{\mathrm{b}}T/4\zeta)(l/R_{ij})\left[\left(\delta_{\alpha\beta} + \frac{{R_{ij}}^{\alpha}{R_{ij}}^{\beta}}{{R_{ij}}^2}\right) + \frac{2a^2}{3{R_{ij}}^2}\left(\delta_{\alpha\beta} - \frac{3{R_{ij}}^{\alpha}{R_{ij}}^{\beta}}{{R_{ij}}^2}\right)\right] \tag{11a}$$

for $R_{\mathrm{ij}} = |\vec{R}_{ij}| = |\vec{r}_i - \vec{r}_j| \geq 2a$ and

$$D_{ij}^{\alpha\beta} = (k_{\mathrm{b}}T/\zeta)\left[\left(1 - \frac{9R_{ij}}{32a}\right)\delta_{\alpha\beta} + \frac{3}{32a}\frac{{R_{ij}}^{a}{R_{ij}}^{\beta}}{{R_{ij}}^2}\right] \tag{11b}$$

for $R_{ij} < 2a$, where $R_{ij}$ is the distance between the $i$th and $j$th beads with the hydrodynamic radius $a$. The strength of the HI is defined by the parameter $h = (3/\pi)^{1/2}\zeta/(6\pi\eta_{\mathrm{s}}l)$, where $\eta_{\mathrm{s}}$ is the solvent viscosity. The freely draining model ($h = 0$) and the model with HI ($h = 0.25$) have been considered. The last case corresponds to the value of the monomer hydrodynamic radius $a = 0.257l$.[19]

In this study we use dimensionless quantities where length $l$, energy $k_{\mathrm{b}}T$, time $\zeta l^2/k_{\mathrm{b}}T$, and translational friction of a single bead $\zeta = 6\pi\eta_{\mathrm{s}}a$ are set to unity. The dimensionless integration step is equal to $\Delta t = 10^{-4}$. This value of $\Delta t$ was chosen to have the maximum displacement of a bead less than 10% of the bond length.

To keep the bond length at some fixed distance $l$ the SHAKE algorithm[28] is used with the tolerance $T = 2 \times 10^{-6}$.

To generate the initial configuration of a dendrimer the procedure suggested by Murat and Grest[16] was used here. Generation $g = 0$ is created by attachment of $b = 3$ chains of $s = 1$ monomers each to the core at three randomly chosen points. Each bead is connected to the similar one by rigid bond $l$. The next generation is made by adding of $b - 1$ bonds to each of the terminal beads of the previous generation. The distance $r$ between the last added monomer and all monomers of the previous generations was chosen as $r \geq r_{\mathrm{min}} = 0.8\sigma$ to avoid the beads overlapping. If a bead cannot be inserted after 500 trials, the whole dendrimer is discarded, and the process is started again with a new random-number seed.

After the generation of the initial configuration, a dendrimer was equilibrated for $5 \times 10^5$−$10^6$ time steps. The length of the equilibration procedure depends on the size of a dendrimer and on the salt concentration in solution. The equilibration was controlled by measuring the instant values of the squared gyration radius, ${R_{\mathrm{g}}}^2$. The length of the equilibration procedure was 2 orders of magnitude larger than the characteristic relaxation time of the correlation function $C_{{R_{\mathrm{g}}}^2}(t)$ for the squared gyration radius (see eq 19 below). After the equilibration, 9−11 production runs of $10^6$ integration steps each have been performed. The final configuration of each run served as the starting configuration of the next run. The calculated statistical characteristics have been obtained by averaging the results through all production runs.

## 3. Dynamical Properties

All dendrimer motions may be divided into three main types: (1) translational and orientational motions of a dendrimer as a whole (global motions); (2) fluctuations of the dendrimer size and shape (elastic motions); (3) local motions with scales corresponding to the length of only a few monomer units. These types of motions will be discussed separately in the following sections of the paper.

**3.1. Global Motions. 3.1.1. Translational Self-Diffusion.** To study the translational diffusion of a dendrimer, we calculated the time dependence of the mean-squared displacement $\langle \Delta {r_{\mathrm{C}}}^2(t)\rangle$ of its center of mass. The self-diffusion coefficient $D$ of a dendrimer as a whole can be estimated from the slope of this dependence as

$$D = \frac{1}{6}\frac{\mathrm{d}\langle \Delta {r_{\mathrm{C}}}^2(t)\rangle}{\mathrm{d}t} \tag{12}$$

for the displacements exceeding the squared gyration radius, $\langle \Delta {r_{\mathrm{C}}}^2(t)\rangle > {R_{\mathrm{g}}}^2$. In this region the dependence of $\langle \Delta {r_{\mathrm{C}}}^2(t)\rangle$ is linear with time for neutral and charged dendrimers (see Figure 1 for neutral dendrimers). Due to the limitation of the CPU time, we have succeeded to obtain reliable data in this region only up to $g = 3$ and $g = 4$ dendrimers for a free-draining model and a model with HI, correspondingly.

The simulated dependence of the self-diffusion coefficient $D$ vs $1/N$ for a free-draining model and for a

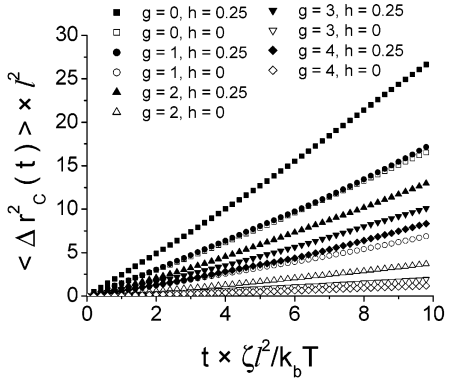


**Figure 1.** Time dependence of the mean-squared displacement $\langle \Delta r_C^2(t) \rangle$ of the center of mass for neutral $g = 0-4$ dendrimers.

model with HI are plotted in Figure 2a. Here and further the error bars are within the size of the symbols which are used to represent the simulated data. For a Brownian particle with translational friction coefficient $\zeta_{self}$ $D$ is equal to $(k_bT/\zeta_{self})$. For a free-draining model of a dendrimer $\zeta_{self}$ is a sum of the friction coefficients $\zeta$ of $N$ beads,

$$\zeta_{self} = N\zeta \tag{13}$$

and $D = (k_bT/N\zeta)$. Indeed, the slope of the simulated dependence $D(1/N)$ for a free-draining model is close to unity, Figure 2a.

For a model with HI the simulated values of $D$ are larger than for a free-draining one. The slope of the dependence of $D$ vs $1/N$ is approximately equal to 0.35. It is related to the partial dragging of the solvent by the moving molecule due to the presence of HI. If a dendrimer can be considered as an impenetrable sphere of radius $R_h$ (hydrodynamic radius of the dendrimer), the friction coefficient $\zeta_{self}$ is described by Stokes' equation (remember that $\zeta = 6\pi\eta a = 1$ in our model):

$$\zeta_{self} = 6\pi\eta R_h = R_h/a \tag{14}$$

Using eq 14, the hydrodynamic radius could be independently calculated from the BD data for the diffusion coefficient. It occurs that $R_h$ is smaller than $R_g$, Table 1. For a dense spherical particle the hydrodynamic radius $R_h$ should be proportional to the gyration radius $R_h \sim R_g = \sqrt{\langle R_g^2 \rangle}$. The dependence of $D$ vs $1/R_g$ is plotted in Figure 2b, where a power-law dependence with a slope 0.8 instead of unity is observed $(R_h \sim R_g^{0.8})$.

**Table 1. Values of the Hydrodynamic Radius $R_h$ and the Average Radius of Gyration $R_g = \sqrt{\langle R_g^2 \rangle}$ for Dendrimers with Hydrodynamic Interactions**

| $g$ | $R_h$ | $R_g$ |
|---|---|---|
| 0 | $0.57 \pm 0.02$ | $0.79 \pm 0.02$ |
| 1 | $0.86 \pm 0.03$ | $1.26 \pm 0.03$ |
| 2 | $1.08 \pm 0.05$ | $1.74 \pm 0.05$ |
| 3 | $1.33 \pm 0.07$ | $2.24 \pm 0.07$ |

As was shown by Ganazzoli et al.,[29] the condition of $R_h < R_g$ is valid both for ideal (without excluded-volume interactions) dendrimers and for dendrimers in a good solvent. This result was obtained in the framework of a self-consistent free-energy minimization with the hydrodynamic radius $R_h$ calculated using the Zimm approach with preaveraged HI. Cai and Chen[13] have calculated the diffusion coefficient $D$ for a dendrimer model with a hard-core interparticle potential and preaveraged HI (MC simulation was used in ref 13 also to carry out the thermodynamical averaging). It was shown that the value of $D$ depends on the ratio $d^2/l^2$, where $d$ is the diameter of a bead. In our model we can put $d \approx \sigma$ and $d^2/l^2 = 0.64$. At $d^2/l^2 = 0.5$, theory[13] predicts a $g$-dependence of $D$ close to that from this study (Figure 3).

The self-diffusion coefficient of dendrimers was calculated also with MD simulation by Karatasos et al.[17] They considered a dendrimer model in a solvent corresponding to the $\theta$-conditions for a linear chain, with spacers consisting of two elastic springs. The ratio $d/l$ was chosen close to unity. Scaling relation $D \sim N^{-0.5}$ was obtained in agreement with the Zimm theory[13] for the value of $d/l \approx 1$ (instead of $D \sim N^{-0.35}$ in this study, where $d/l = 0.8$). Therefore, we can conclude that the dependence of the diffusion coefficient $D$ on the generation number agrees well with predictions of the preaveraged Zimm approach. The difference in the numerical values can be explained by the difference in the form of the excluded volume potentials (hard-core potential in the Zimm theory[13] and soft Lennard-Jones potential in this study).

Rietveldt and Bedeaux[30] determined the self-diffusion coefficient $D_0$ in a very dilute solution of up to $g = 5$ generations poly(propylene imine) dendrimers in methanol by NMR method. The power law $D_0 \sim N^{-\alpha}$ has been obtained in ref 30 with $\alpha = 0.36$ at $T = 40$ °C and $\alpha = 0.38$ at $T = 25$ °C. At $T = 5$ °C the fit of their data gives $\alpha = 0.32$. The recent NMR results of Baille et al.[31] give $\alpha = 0.40$ for dilute solutions of poly(propylene imine) dendrimers in poly(vinyl alcohol) at $T = 25$ °C and $\alpha = 0.39$ at $T = 5$ °C. Thus, the molecular-weight depen-

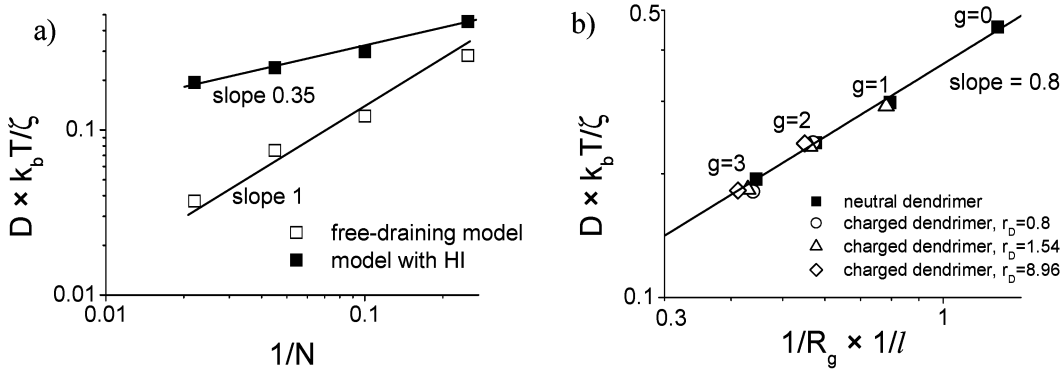


**Figure 2.** Self-diffusion coefficient $D$ for (a) the free-draining model and model with HI, neutral dendrimers, as a function of $1/N$ and for (b) the model with HI, $h = 0.25$, neutral and charged dendrimers, as a function of $1/R_g$.

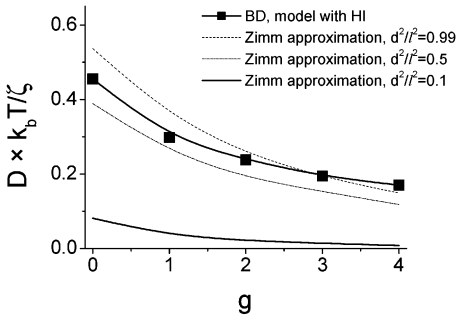


**Figure 3.** Dependence of the self-diffusion coefficient $D$ of neutral dendrimers on the generation number for a model with HI. Results of Cai and Chen[13] for a dendrimer with excluded-volume interactions and preaveraged HI (Zimm approximation) at different values of ratio $d^2/l^2$ are shown also.

dence of the simulated self-diffusion coefficients from this study is in a very good quantitative agreement with known experimental results.

For a free-draining model the self-diffusion coefficient for charged dendrimers coincides with that for neutral ones as expected. For a model of a charged dendrimer with HI the values of $D$ decrease a little, but the relationship $R_h \sim R_g^{0.8}$ remains to be valid.

**3.1.2. Rotation of a Dendrimer as a Whole.** The rotational mobility of a dendrimer as a whole can be characterized by the correlation function $C_{rot}(t)$

$$C_{rot}(t) = \langle \vec{e}_g(0)\vec{e}_g(t)\rangle \tag{15}$$

where $\vec{e}_g = (\vec{Q}_g/|\vec{Q}_g|)$ is a unit vector directed along the position vector $Q_g$ for terminal monomers with respect to the core:

$$\vec{Q}_g = \vec{r}_t - \vec{r}_0 \tag{16}$$

Here $\vec{r}_t$ represents the position of an arbitrary terminal $t$th monomer for a $g$-generation dendrimer and the vector $\vec{r}_0$ represents the position of the dendrimer core. Averaging in eq 15 is performed over all terminal groups.

Figure 4a illustrates a typical time dependence of $C_{rot}(t)$ for $g = 4$ dendrimers. The time dependence of ln $C_{rot}(t)$ is close to linear. The relaxation times $\tau_{rot}$ of $C_{rot}(t)$ are determined as $C_{rot}(\tau_{rot}) = 1/e$ and shown in Figure 4b. Relaxation times increase with increase of the generation number. For a solid spherical body with radius $R$ in a viscous medium $\tau_{rot} \sim R^3$. For a dendrimer model with HI we obtain the same result when $R$ is taken to be equal to $R_g$. For charged dendrimers the time $\tau_{rot}$ is slightly larger reflecting some swelling of a dendrimer under charging.

**3.1.3. Relaxation of a Monomer-to-Core Vector.** Cai and Chen[12,13] considered the relaxation of a monomer-to-core vector $\vec{Q}_g$. The corresponding correlation function is defined as

$$C_Q(t) = \frac{\langle \vec{Q}_g(0)\vec{Q}_g(t)\rangle}{\langle Q_g^2\rangle} \tag{17}$$

The characteristic relaxation times $\tau_r$ for the function $C_Q(t)$ were calculated. For an ideal dendrimer (Rouse model) the following expression was derived:

$$\tau_r = 2^{g+2}\zeta/K \tag{18}$$

Here $K$ is the effective force constant for a spring connecting two neighboring branching points ($K = 3k_bT/l^2$, $l^2$ is the mean-squared distance between branching points) and $\zeta$ is the monomer friction coefficient. The number of monomers $N$ in a generation $g$ dendrimer is proportional to $2^{g+1}$. Therefore, eq 18 predicts the linear dependence $\tau_r$ vs $N$. Note that for a Rouse model of a linear chain with $N$ monomers the relaxation time of an end-to-end vector scales as $N^2$. For a dendrimer with HI Cai and Chen calculated these times by using the preaveraged Zimm approach.[13] The dependence $\tau_r$ vs $N$ for $d/l = \sqrt{0.5}$ is shown in Figure 5a. The log−log dependence is linear with slope ~1.1, a little larger than for an ideal dendrimer.

We calculated correlation functions $C_Q(t)$ for our model, Figure 4a. Values of $\tau_r$ for neutral dendrimers with and without HI are shown in Figure 5a. For a free-draining model of dendrimers with excluded-volume interactions we obtained the dependence $\tau_r \sim N^{1.6}$, Figure 5a, as compared to the much weaker dependence $\tau_r \sim N$ obtained by Cai and Chen[12] for an ideal dendrimer. The weaker molecular-weight dependence of the relaxation time $\tau_r$ obtained by Cai and Chen is probably related to the absence of the excluded-volume interactions in their phantom model.[12]

BD simulation of dendrimers with HI gives a weaker dependence of $\tau_r$ vs $N$, $\tau_r \sim N^{1.3}$, as compared to the free-draining case, but stronger than that predicted by Cai and Chen[13] (Figure 5a).

To understand the origin of the difference between the calculations of Cai and Chen[12,13] and simulated

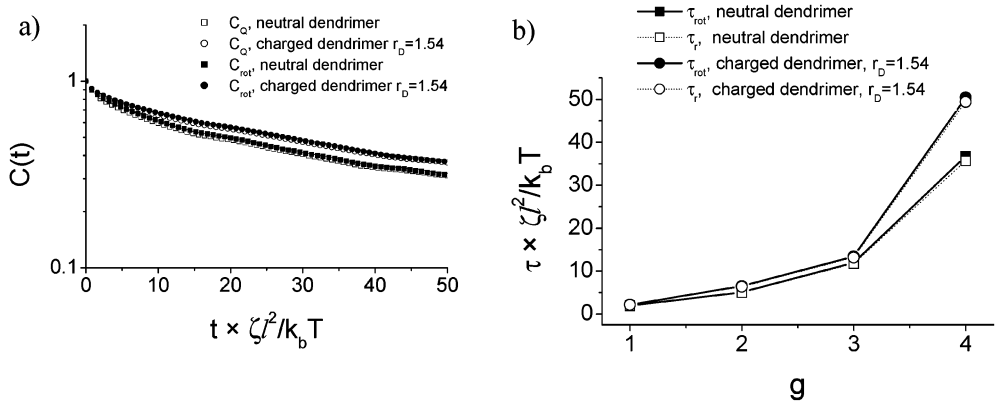


**Figure 4.** (a) Time dependence of the correlation functions $C_{rot}(t)$ and $C_Q(t)$ for $g = 4$ dendrimer, model with HI. **(**b) Dependence of the relaxation times $\tau_{rot}$ and $\tau_r$ on the generation number $g$, model with HI. Lines connecting symbols are drawn as a guide to the eye.

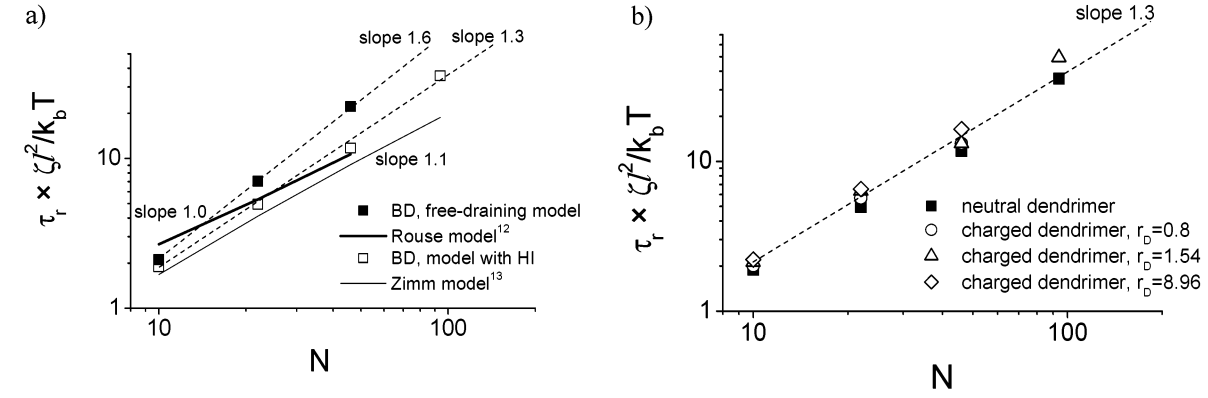


**Figure 5.** Dependence of the relaxation time $\tau_r$ on the total number of monomers (a) for the free-draining model and model with HI with neutral dendrimers (results of Cai and Chen[12,13] shown by solid lines; value of $d/l = 0.5$ chosen for the model with HI) and (b) for the charged dendrimers with different Debye lengths, model with HI.

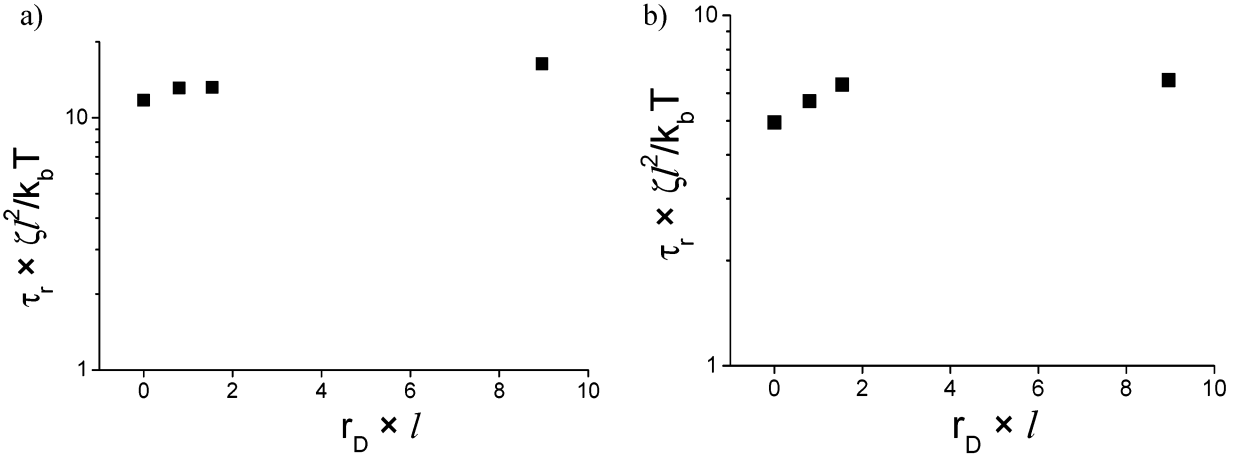


**Figure 6.** Dependence of the relaxation time $\tau_r$ on Debye length $r_D$ for charged (a) $g = 2$ and (b) $g = 3$ dendrimers, model with HI. The value of the relaxation time is almost constant at $r_D \geq 2$.

values of $\tau_r$ in this paper, one has to have in mind that the relaxation of $\tau_r$ is due to the rotation of a dendrimer as a whole and due to the internal motions. Comparison of the simulated values of $\tau_r$ and $\tau_{er}$ for neutral dendrimers shows that they coincide both for a free-draining model and a model with HI, Figure 4b. Thus, the relaxation of a monomer-to-core vector in our model is determined by the rotation of a dendrimer as a whole. Cai and Chen[12,13] used dendrimer models with flexible spacers for which the contribution of internal motions to the relaxation of a monomer-to-core vector is significant. That is why for dendrimers with flexible spacers a weaker dependence $\tau_r(N)$ is observed as compared to the dendrimer with rigid spacers in this study, Figure 5a.

For charged dendrimers with HI relaxation times $\tau_r$ also coincide with $\tau_{er}$ (see Figure 4b for $r_D = 1.54$). These times weakly increase with the increase of $r_D$, achieving saturation at large $r_D$, Figure 6. However, the value of the exponent $\nu \sim 1.3$ in the dependence $\tau_r \sim N^\nu$ is found to be the same as for the neutral dendrimers, Figure 5b.

**3.2. Dendrimer Elastic Motions. 3.2.1. Autocorrelation Function of the Gyration Radius.** The dynamics of the fluctuations of the dendrimer size can be characterized by the correlation function $C_{R_g^2}(t)$ for the squared radius of gyration:

$$C_{R_g^2}(t) = \frac{\langle R_g^2(0) R_g^2(t)\rangle - \langle R_g^2\rangle^2}{\langle R_g^4\rangle - \langle R_g^2\rangle^2} \qquad (19)$$

The relaxation of $C_{R_g^2}(t)$ occurs only due to the internal motions; the rotation of a dendrimer as a whole does not contribute to the relaxation of $C_{R_g^2}(t)$. Figure 7a illustrates a typical time dependence of $C_{R_g^2}(t)$ for neutral $g = 1-3$ dendrimers. The time dependence of $\ln C_{R_g^2}(t)$ is close to linear.

Characteristic times $\tau_{R_g^2}$ determined as $C_{R_g^2}(\tau_{R_g^2}) = e^{-1}$ are shown in Figure 7b. The relaxation times $\tau_{R_g^2}$ are significantly smaller than $\tau_r$ (Figure 5). Murat and Grest[16] in their MD study also obtained that $\tau_{R_g^2} < \tau_r$. At the same time for the models considered by Cai and Chen with and without HI[12,13] $\tau_{R_g^2}$ coincides with $\tau_r$. For the free-draining model of a dendrimer[12] the equality $\tau_{R_g^2} = \tau_r$ is related to the fact that the phantom viscoelastic model without excluded-volume interaction was used. For the model with preaveraged HI and excluded-volume interactions Cai and Chen[13] noted that the equality $\tau_{R_g^2} = \tau_r$ is an artifact of the theory due to the use of a linearized version of the Langevin equation and $\tau_{R_g^2}$ should be smaller than $\tau_r$ in the real dendrimer systems. Results of the present BD simulations confirm this conclusion. It is interesting to note that in contrast to the predictions of Cai and Chen[12,13] the simulated times are not changed significantly by taking into account HI explicitly. It means that the relaxation times

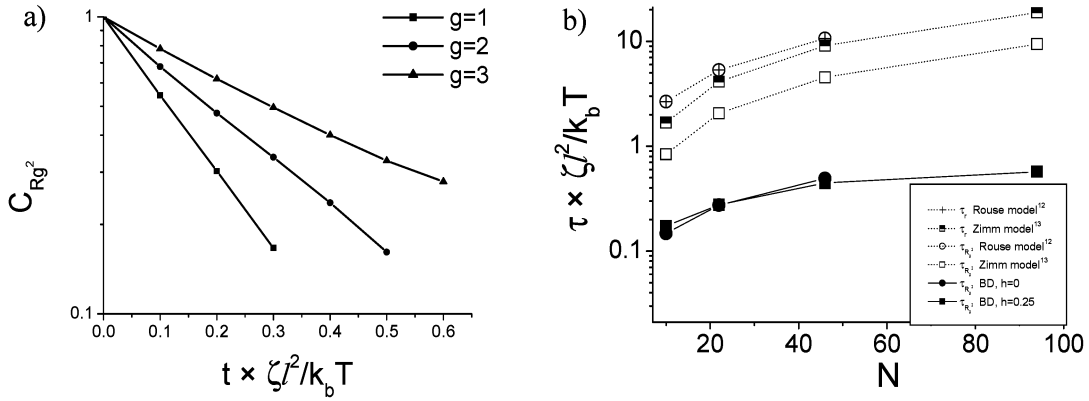


**Figure 7.** (a) Time dependence of correlation function $C_{R_g^2}(t)$ for neutral $g = 1-3$ dendrimers, model with HI. (b) Dependence of the relaxation time $\tau_{R_g^2}$ on number of monomers $N$ for neutral dendrimers. Dependence of $\tau_r(N)$ and $\tau_{R_g^2}(N)$ obtained by Cai and Chen[12,13] for the model without and with HI and excluded-volume interactions is also shown.

$\tau_{R_g^2}$ are related to the local motions in a dendrimer, which, as will be shown below, weakly depend on HI.

The dependence of the relaxation times $\tau_{R_g^2}$ on the number of monomers $N$ is weaker than that predicted by Cai and Chen,[12,13] Figure 7b. Weak (especially for large values of $N$) dependence $\tau_{R_g^2}(N)$ agrees with the BD simulation results for neutral dendrimers.[19] The relaxation times obtained in neutron-scattering experiments of Stark et al.[8] for carbosilane dendrimers as well as the relaxation times estimated from the times $T_1$ and $T_2$ in NMR experiments for PAMAM dendrimers[10−11] also show weaker dependence on $g$ in comparison to the predictions of Cai and Chen.[12,13]

Weak dependence $\tau_{R_g^2}(N)$ for a model with HI can be understood if we consider the dendrimer as an elastic spherical body in a viscous medium. The characteristic times $\tau_{sph}$ of the shape relaxation can be written in this case as

$$\tau_{sph} = \frac{\zeta}{K} \tag{20}$$

where $\zeta \sim R$ and $K$ are the friction and the elasticity coefficients, respectively. It is easy to show that $K \sim ER$, where $E$ is the Young modulus. Therefore, the large-$g$ dendrimer with HI may be considered as an impenetrable sphere, and $\tau_{sph}$ does not depend on $R$ in agreement with the results from this study. For a free-draining dendrimer such a model predicts larger values of $\tau_{R_g^2}(N)$ as compared to those for a model with HI due to the increased friction coefficients. Simulation results agree with this prediction, Figure 7b. The simulation data have been collected only for the low-$g$ dendrimers, and a definite conclusion about the dependence $\tau_{R_g^2}(R)$ is difficult to make.

For charged dendrimers increasing of the Debye length leads to decreasing of the relaxation time $\tau_{R_g^2}$, Figure 8. Electrostatic repulsion increases the internal strain and, therefore, effective rigidity of a dendrimer, which, in turn, leads to a decrease of the corresponding characteristic times, Figure 8.

**3.2.2. Relaxation of Fluctuations of the Center-of-Mass-to-Core Vector.** Cai and Chen[12] considered the relaxation of fluctuations of the center-of-mass-to-core vector $\vec{S}$

$$\vec{S} = \frac{1}{N+1}\sum_{i=0}^{N}(\vec{r}_i - \vec{r}_0) \tag{21}$$

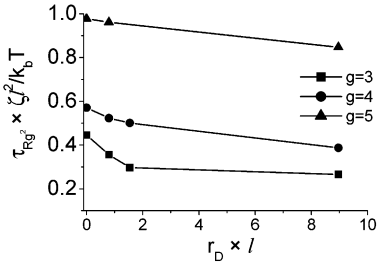


**Figure 8.** Dependence of the relaxation time $\tau_{R_g^2}$ on the Debye screening length for $g = 3-5$ dendrimers, model with HI.

The corresponding autocorrelation function $C_S$ is defined as

$$C_S(t) = \frac{\langle \vec{S}(0)\vec{S}(t)\rangle}{\langle S^2\rangle} \tag{22}$$

and characterized by the relaxation time $\tau_{com}$. The approximate expression for $\tau_{com}$ for the free-draining Rouse model of a dendrimer[12] was derived as $\tau_{com} \sim \zeta/((3/l^2)(3 - 2\sqrt{2}\cos(\pi/(g+1))))$. We examine the function $C_S$ for the models in this study. The corresponding values of $\tau_{com}$ vs $g$ are plotted both for neutral, Figure 9a, and charged, Figure 9b, dendrimers. To compare the results of BD simulation with the theoretical predictions a mean-squared spacer length $l^2$ in the expression for $\tau_{com}$ was taken equal to the squared bond length. A drastic difference is seen between the theoretical and simulated dependence, Figure 9a. The Rouse model predicts a practically linear increase of $\tau_{com}$ with the generation number $g$. Simulated relaxation times $\tau_{com}$ at small $g$ are larger than theoretical ones and then go through the maximum and decrease at larger $g$. It is interesting that the simulated relaxation times show the similar behavior for dendrimers both with and without HI. For charged dendrimers the character of the dependence $\tau_{com}(g)$ remains qualitatively the same, but all times decrease with the increase of Debye length, Figure 9b.

We suppose that the difference between the dependences of the relaxation times $\tau_{com}$ vs $g$ obtained in this study and by Cai and Chen[12] is related to the spacer flexibility. For flexible spacers in the Rouse model[12] the increase of the generation number $g$ leads to an increase of the relaxation times $\tau_{com}$ due to the increase of the friction coefficient of the whole dendrimer. For the dendrimer model considered in this study spacers are

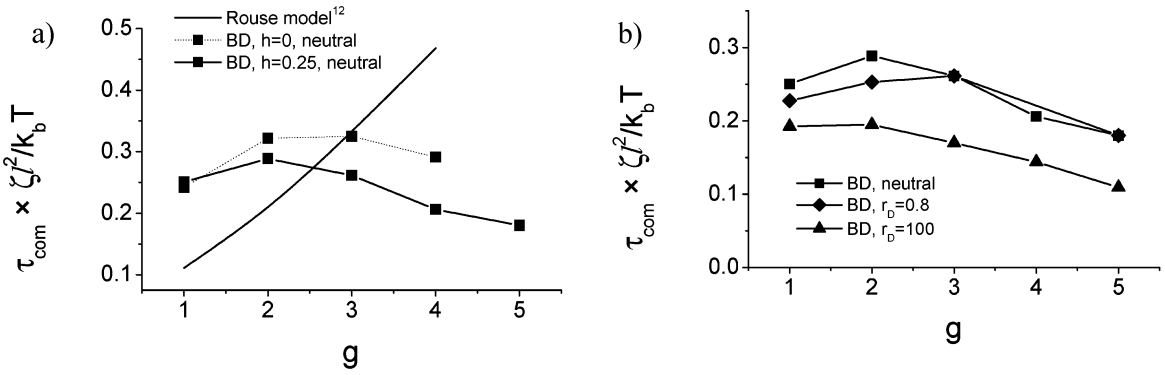


**Figure 9.** Dependence of the relaxation time $\tau_{com}$ on the generation number $g$ both for (a) the neutral, free-draining model and the model with HI and (b) neutral and charged dendrimers, model with HI.

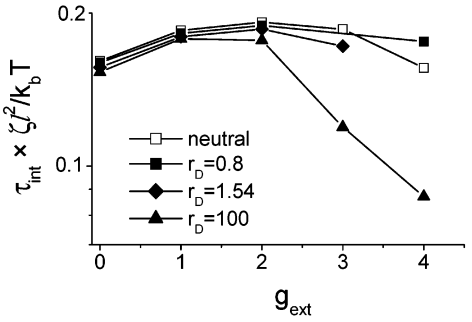


**Figure 10.** Dependence of the "internal pulsation" relaxation time $\tau_{int}$ for the monomers belonging to the generation shell $g_{int} = 1$ on the number of exterior generations $g_{ext}$, model with HI. Solid lines are shown here as guides to an eye.

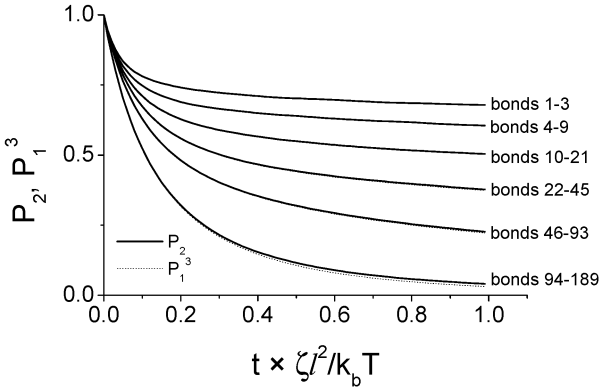


**Figure 11.** Time dependence of the autocorrelation functions $P_2$ and $P_1^3$ for a neutral $g = 5$ dendrimer, model with HI. Bonds 1−3 are attached to the core, and bonds 94−189 are the terminal bonds of a $g = 5$ dendrimer.

rigid. So, the increase of the generation number leads also to the increase of the internal strain in the dendrimer. That is why the dependence of the relaxation times $\tau_{com}$ on the generation number $g$ is nonmonotonic, Figure 9.

**3.3. Local Dynamics. 3.3.1. Internal "Pulsations".** It is interesting to consider the motions of monomers belonging to the same generation shell $g_{int}$ inside the $g$ generation dendrimer. The dynamics of these internal "pulsations" in a dendrimer can be characterized by the correlation function $C_{g_{int}}$ for the squared distance $h_i^2 = (\vec{r}_i - \vec{r}_0)^2$ between a core $\vec{r}_0$ and the monomers with position $\vec{r}_i$ of a given generation shell inside the dendrimer:

$$C_{g_{int}} = \frac{1}{N_{g_{int}}} \sum_i \frac{\langle h_i^2(0) h_i^2(t)\rangle - \langle h_i^2\rangle^2}{\langle h_i^4\rangle - \langle h_i^2\rangle^2} \qquad (23)$$

Here $N_{g_{int}}$ is the number of beads in the corresponding generation shell. Simulated characteristic times $\tau_{int}$ for this function for $g_{int} = 1$ in dendrimers with different number of exterior generations $g_{ext} = g - g_{int}$ are shown in Figure 10. Relaxation times $\tau_{int}$ do not depend on the number of exterior generations. Only for large values of the Debye length $\tau_{int}$ decreases with increase of $g_{int}$. Additional stretching of a dendrimer due to the electrostatic repulsion between charged terminal monomers leads to the decrease of the fluctuations of internal motions and to the faster decrease of $\tau_{int}$. It would be interesting to study the influence of the number of exterior generations on the pulsations of more distant shells, $g_{int} > 1$. For this purpose the simulations of larger dendrimers are necessary.

**3.3.2. Local Orientational Mobility.** The local orientational mobility of a single bond inside the dendrimer can be probed by the orientational autocorrelation functions $P_1$ and $P_2$

$$P_1(t) = \langle \vec{b}_i(0)\vec{b}_i(t)\rangle \qquad (24)$$

$$P_2(t) = \frac{3}{2}\left(\langle \vec{b}_i(0)\vec{b}_i(t)\rangle^2 - \frac{1}{3}\right) \qquad (25)$$

where $\vec{b}_i(t)$ is the unit vector directed along the $i$th bond.

For a single rigid dumbbell there is a simple relation between $P_1$ and $P_2$:[32]

$$P_2(t) = P_1^3(t) \qquad (26)$$

This relation turns out to be valid for all monomers inside both neutral and charged dendrimers, without and with HI (see as example Figure 11 for the model with HI).

In what follows we analyze the behavior of $P_1(t)$ only. Results of the BD simulations show that changing of the Debye length, Figure 12, and the presence of hydrodynamic interactions, Figure 13, affect mainly the orientational behavior of the bonds of the first generation shell (bonds which are directly attached to the core). Such an influence becomes weaker for the bonds of all other generations. Existence of HI leads to the faster relaxation, Figure 13. Influence of the HI becomes stronger for the dendrimers of large generation number ($g > 3$). Increase of the Debye length leads to slower relaxation of $P_1$, Figure 12. We suppose that two processes contribute to the relaxation of $P_1$. The initial

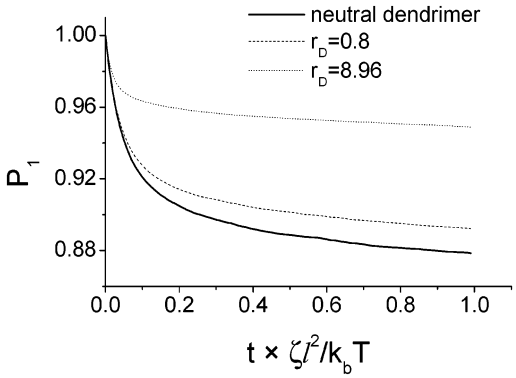


**Figure 12.** $P_1$ autocorrelation function for the bonds attached to the core of a $g = 5$ dendrimer at different values of Debye length, model with HI.

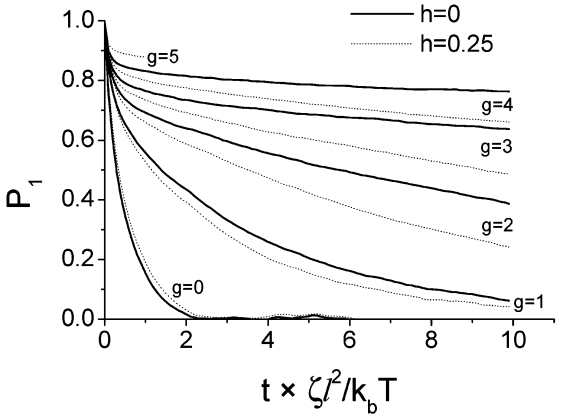


**Figure 13.** $P_1$ autocorrelation function for the bonds attached to the core for neutral dendrimers of different generations with and without HI.

stage of the relaxation (up to $t \sim 0.1-0.2$) may be determined by the fast internal "pulsation" motions of monomers. The final part of the relaxation is related to the global rotation of the dendrimer as a whole.

The maximum rate of the $P_1(t)$ relaxation is observed for the terminal groups, Figure 14. With the exception of $g = 0$ dendrimer, the shape of $P_1(t)$ is similar for dendrimers of different generations and HI does not influence the $P_1(t)$ relaxation of these groups, Figure 14a.

MD simulations of Karatasos et al.[17] for a dendrimer with spacer length $s = 2$ also show the independence of the orientational mobility of terminal groups on the dendrimer size up to generation $g = 6$. A small sensitivity of the rotational mobility of the terminal groups to the number of generations was demonstrated experimentally by Stark et al.[8] for dendrimers with perfluorinated terminal groups. For a charged dendrimer $P_1(t)$ for terminal groups also does not depend on the total number of generations. Weak deceleration of $P_1(t)$ relaxation is observed with increase of the Debye length (see Figure 14b for $g = 5$ dendrimer). Such a behavior can be explained by the stretching of a dendrimer due to the electrostatic repulsion which leads to an increase of the interconnection between the orientational motions of terminal groups and a rotation of a dendrimer as a whole.

## 4. Conclusions

The BD simulation of neutral and charged dendrimers of generations $g = 0-5$ with rigid spacers between branching points and explicit hydrodynamic and excluded-volume interactions has been carried out. The molecular-mass dependence of the self-diffusion coefficient of neutral dendrimers is in a satisfactory agreement with theoretical predictions for the model with preaveraged HI[13] and in a very good quantitative agreement with recent NMR results[30,31] for dilute solutions of poly(propylene imine) dendrimers. Due to the rigid character of the dendrimer model increase of the scale of electrostatic interactions (Debye length) does not lead to a significant change of the translational mobility of a dendrimer as a whole. The hydrodynamic radius both for neutral and charged dendrimers turns out to be less than gyration radius.

Dynamics of the size fluctuations for a dendrimer with rigid spacer differs principally from the theoretical predictions for a dendrimer with flexible spacers. The relaxation of these fluctuations is weakly sensitive to the presence of HI and turns out to be considerably faster. The dendrimer behavior is close to that of an elastic body in a viscous medium. Electrostatic interactions increase the internal strain and effective rigidity of a dendrimer, which, in turn, lead to a decrease of the corresponding characteristic relaxation times. It would be interesting to simulate the dynamics of dendrimers of larger generations with longer and more flexible spacers in the future. One could expect some increase of the relaxation time $\tau_{R_g^2}$ for neutral dendrimers and stronger effect of electrostatic interactions with an increase of spacer flexibility.

Orientational mobility of bonds corresponding to the different generations of shells inside the dendrimer increases from the core to the periphery. Mobility of the terminal groups does not depend on the generation number, in agreement with the neutron-scattering experimental results[8] for carbosilane dendrimers. For the rigid dendrimer model of this study the mobility of

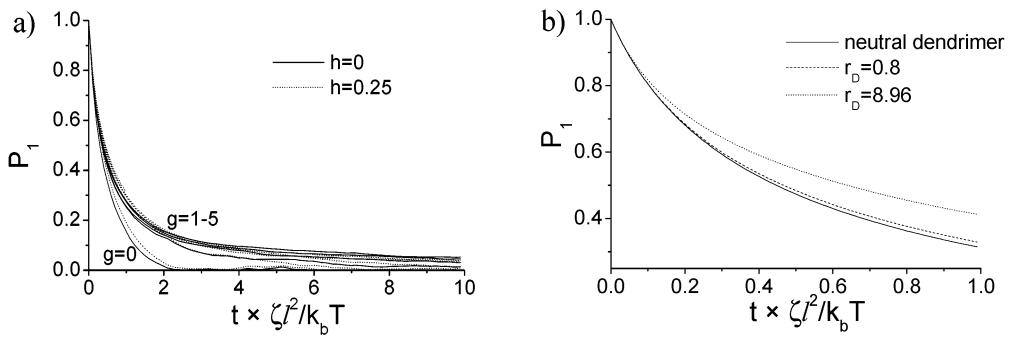


**Figure 14.** $P_1$ autocorrelation function for terminal groups of (a) neutral $g = 0-5$ dendrimers, $h = 0.25$, and $h = 0$ and of (b) neutral and charged $g = 5$ dendrimer, $h = 0.25$, with different values of Debye length.

the terminal bonds is weakly sensitive to the value of the Debye length. For flexible dendrimers we also expect higher sensitivity of this type of motion to the strength of electrostatic interactions.

**Acknowledgment.** The authors are grateful to Dr. I. Neelov for his help in performing some production runs. This work was carried out with the financial support of the NWO Grant 047.009.017, ESF programs SIMU, SUPERNET, RFBR Grants 02-03-33135 and 03-03-06379, and INTAS Grant 00-712.

## References and Notes

(1) Liu, M. J.; Frechet, M. J. *Pharm. Sci Technol. Today* **1999**, *2*, 393.
(2) Jansen, J. F. G. A.; de Brabander-van den Berg, E. M. M.; Meijer, E. W. *Science* **1994**, *266*, 1226.
(3) Service, R. *Science* **1995**, *267*, 458.
(4) Szoka, F. C.; Haensler, Jr.; Haensler, J. (University of California). U.S. Patent 93-92200.
(5) De Gennes, P. G.; Hervet, H. *J. Phys., Lett.* **1983**, *44*, 351.
(6) Welch, P.; Muthukumar, M. *Macromolecules* **1998**, *31*, 5892.
(7) Welch, P.; Muthukumar, M. *Macromolecules* **2000**, *33*, 6159.
(8) Stark, B.; Stuhn, B.; Frey, H.; Lach, C.; Lorenz, K.; Frick, B. *Macromolecules* **1998**, *31*, 5415.
(9) Emran, S. K.; Newkome, G. R.; Weis, C. D.; Harmon, J. P. *J. Polym. Sci., Part B: Polym. Phys.* **1999**, *37*, 2025.
(10) Meltzer, D.; Tirrel, D. A.; Jones, A. A.; Inglefield, P. T.; Hedstran, D. M.; Tomalia, D. A. *Macromolecules* **1992**, *25*, 4541.
(11) Meltzer, D.; Tirrel, D. A.; Jones, A. A.; Inglefield, P. T. *Macromolecules* **1992**, *25*, 4549.
(12) Cai, Ch.; Chen, Zh. Yu. *Macromolecules* **1997**, *30*, 5104.
(13) Chen, Zh. Yu.; Cai, Ch. *Macromolecules* **1999**, *32*, 5423.
(14) Ganazzoli, F.; La Ferla, R.; Raffaini, G. *Macromolecules* **2001**, *34*, 4222.
(15) Boris, D.; Rubinstein, M. *Macromolecules* **1996**, *29*, 7251.
(16) Murat, M.; Grest, G. *Macromolecules* **1996**, *29*, 1278.
(17) Karatasos, K.; Adolf, D. B.; Davies, G. R. *J. Chem. Phys.* **2001**, *115*, 5310.
(18) Lee, I.; Athey, B. D.; Wetzel, A. W.; Meixner, W.; Baker, J. R. *Macromolecules* **2002**, *35*, 4510.
(19) Lyulin, A. V.; Davies, G. R.; Adolf, D. B. *Macromolecules* **2000**, *33*, 3294.
(20) Lyulin, A. V.; Davies, G. R.; Adolf, D. B. *Macromolecules* **2000**, *33*, 6899.
(21) Lyulin, A. V.; Adolf, D. B.; Davies, G. R. *Macromolecules* **2001**, *34*, 3783.
(22) Lyulin, A. V.; Adolf, D. B.; Davies G. R. *Macromolecules* **2001**, *34*, 8818.
(23) Lyulin S. V.; Evers, L. J.; van der Schoot, P.; Darinskij, A. A.; Lyulin A. V.; Michels, M. A. J. *Macromolecules* **2004**, *37*, 3049.
(24) Ermak, D. L.; McCammon, J. A. *J. Chem. Phys.* **1978**, *69*, 1352.
(25) van Duijvenbode, R. C.; Borkovec, M.; Koper, G. J. M. *Polymer* **1998**, *39*, 2657.
(26) Nisato, G.; Ivkov, R.; Amis, E. J. *Macromolecules* **1999**, *32*, 5895.
(27) Rotne, J.; Prager, S. *J. Chem. Phys.* **1969**, *50*, 4831.
(28) Ryckaert, J.-P.; Bellemans, A. *Chem. Phys. Lett.* **1975**, *30*, 123.
(29) Ganazzoli, F.; la Ferla, R.; Terragni, G. *Macromolecules* **2000**, *33*, 6611.
(30) Rietveldt, I. B.; Bedeaux, D. *Macromolecules* **2000**, *33*, 7912.
(31) Baille, W. E.; Malveau, C.; Zhu, X. X.; Kim, Y. H.; Ford, W. T. *Macromolecules* **2003**, *36*, 839.
(32) Gotlib, Yu. Ya.; Balabaev, N. K.; Darinski, A. A.; Neelov, I. M. *Macromolecules* **1980**, *13*, 602.

MA0357927